Split-HaloTag® Imaging Assay for *in vivo* 3D-Microscopy and Subdiffractional Analyses of Protein-Protein Interactions

Rieke Meinen[1], Jan-Niklas Weber[1], Andreas Albrecht[2], Rainer Matis[2], Maria Behnecke[1], Cindy Tietge[1], Stefan Frank[1], Jutta Schulze[1], Henrik Buschmann[3], Peter Jomo Walla[2], Ralf-R. Mendel[1], Robert Hänsch[1,4]* and David Kaufholdt[1]

r.meinen@tu-bs.de, jan-niklas.weber@tu-bs.de, andreas.albrecht@tu-bs.de, r.matis@tu-bs.de, maria.behnecke@dsmz.de, cindy.oettel@tu-bs.de, stefan.frank@tu-bs.de, jutta.schulze@tu-bs.de, Henrik.buschmann@biologie.uni-osnabrueck.de, p.walla@tu-bs.de, r.mendel@tu-bs.de, r.haensch@tu-bs.de, d.kaufholdt@tu-bs.de

[1]Institut für Pflanzenbiologie, Technische Universität Braunschweig, Humboldtstrasse 1, D-38106 Braunschweig, Germany

[2]Institut für Physikalische und Theoretische Chemie, Technische Universität Braunschweig, Hagenring 30.023c, D-38106 Braunschweig, Germany

[3]Botany Department, Universität Osnabrück, Barbara Str. 11, 49076 Osnabrück Germany

[4]Center of Molecular Ecophysiology (CMEP), College of Resources and Environment, Southwest University, Tiansheng Road No. 2, 400715 Chongqing, Beibei District, P.R. China

*author for correspondence: Tel: +49-(0)531-391-5867

Fax: +49-(0)531-391-8128

E-Mail: r.haensch@tu-bs.de

Date of submission: 2020-06-30

Word count total: 4468

Number of Tables: 0

Number of Supplementary Tables: 2

Number of Figures: 4

Number of Supplementary Figures: 0

Running title: Split-HaloTag® Imaging Assay

Highlights

The Split-HaloTag® assay combine for the first time *in planta* a flexible and photostable fluorescence system with a split-reporter system, which enables protein complex analyses with advanced microscope technologies.

Abstract

An ever-increasing number of protein complexes participating in metabolic pathways and of multi-protein intracellular networks is identified in plant cells. Split-GFP based protein-protein interaction assays combine the advantages of *in vivo* interaction studies in native environment with additional visualisation of protein complex localisation. However, fluorescence proteins have several drawbacks for 3D- imaging and super-resolution microscopy: high photobleaching rate during long-term observations, correlation of fluorescence intensity to expression level, blinking behaviour and the tendency to form oligomers. The HaloTag® system was shown to overcome these drawbacks. This reporter is able to form covalent irreversible bonds with synthetic chloralkane ligands. Several stable fluorescence ligands are available like TMR or Oregon Green, which can be used in variable concentrations for optimal fluorescence intensity. Therefore, we established the new Split-HaloTag® imaging assay to enable advanced fluorescence imaging such as single molecule-, subdiffractional polarisation imaging or super-resolution microscopy of protein-protein interactions. This is demonstrated via studies of molybdenum cofactor biosynthesis complex anchoring to filamentous actin. Specific interactions were visualised with 3D- and advanced subdiffractional polarisation microscopy in distinctive manner. Therefore, this assay is a promising new tool for 3D-imaging and super-resolution microscopy of protein-protein interactions in plant cells.

Keywords

advanced microscopy, cytoskeleton, photostable fluorescence dyes, Gateway cloning, Molybdenum cofactor biosynthesis complex, polarisation microscopy, protein-protein interaction, Split-HaloTag® imaging assay

Abbreviations

BiFC: bimolecular fluorescence complementation; FP: fluorescence protein; SPoD: Super-resolution by polarisation demodulation

Introduction

Understanding the cellular biology of plants requires the characterisation of protein-protein interactions. An increasing number of protein networks and substrate channeling pathways were identified (Zitnik *et al*., 2019). Protein fragment complementation assays such as bimolecular fluorescence complementation (BiFC) allow visualisation of protein interactions in living cells (Bhat *et al*., 2006). Non-fluorescent reporter fragments are fused genetically to putative interaction partners and an interaction between the two allows formation of a bimolecular fluorescent complex (Kerppola, 2008). However, fluorescence intensity of fluorescent proteins (FPs) in general as well as for the BiFC complex in particular is directly interlinked with expression levels of fusion proteins. Some additional drawbacks of FPs can severely hamper microscopic analysis: low quantum efficiency, blinking behaviour, a high photobleaching rate during long-term observations (Reck-Petersen *et al.*, 2006), photoswitching (Morisaki and McNally, 2014) as well as the tendency of FPs to form oligomers (Miyawaki *et al*., 2003). These drawbacks are especially unfavourable when using advanced fluorescence microscopy methods such as two-photon, high content, single molecule, subdiffractional polarisation or super-resolution imaging that typically require fluorescence tags of high stability and brightness (Moerner and Kador, 1989; Orrit and Bernard, 1990; Bode *et al*., 2008; Holleboom *et al*., 2014; Liao *et al*., 2010/2011; Godin *et al*., 2014; Loison *et al*., 2018; Camacho *et al*., 2019).

However, self-labelling enzyme tags such as the HaloTag® have been shown to overcome these drawbacks of FPs and are suitable for such microscopy methods and super-resolution imaging (Grimm *et al*., 2015; Lee *et al*., 2010). The HaloTag® System (Promega, https://www.promega.de/) is based on the bacterial haloalkane dehalogenase DhaA (EC 3.8.1.5) from *Rhodococcus rhodochrous* (Liss *et al*., 2015). The tag was modified to form covalent irreversible bonds with synthetic chloralkane ligands (Los *et al*., 2008; England *et al.,* 2015). This covalent bond is formed rapidly under physiological conditions and remains intact even under stringent conditions (Los and Wood, 2007). Numerous ligands are available for the HaloTag® including different fluorescent dyes with extended spectral range and high photostability such as the red fluorescent rhodamine derivative TMR, the green fluorescent Oregon Green or the yellow fluorescent diacetyl derivative of fluorescein DiAcFAM. Furthermore, dyes can be varied in their dosages to either label all or only a few molecules

which is needed for single-molecule tracking approaches. In addition, HaloTag® proteins keep their monomeric structure, so the tag will not lead to oligomerisation of protein fusion partners. The usability of this imaging system was shown successfully *in planta* (Lang *et al.,* 2006).

In 2012, Ishikawa and colleagues identified several split points within the HaloTag® protein and demonstrated its reconstitution ability. These results gave rise to the idea of establishing the Split-HaloTag® imaging assay suitable for protein-protein interaction studies via advanced fluorescence microscopy methods such as single molecule, subdiffractional polarisation, high content, or super-resolution imaging techniques *in planta.* This new approach is particularly useful for characterising protein complex assembly at structural elements including cell membranes or the cytoskeleton. The possibility of using these microscopy techniques will enable to study local formation and dynamics of a given complex with improved details compared to BiFC and conventional confocal laser scanning microscopy. Single-molecule tracking approaches with limited fluorescent dye will enable the tracing of complex mobility at the cytoskeleton or inside the membrane system. In this study, we used the previously described anchoring of the Molybdenum cofactor biosynthesis complex via molybdate insertase Cnx1 to filamentous actin (Kaufholdt *et al*., 2017) for establishing of the new Split-HaloTag® imaging assay. In this way, we demonstrate the advantages of this assay for imaging of *in vivo* protein-protein interactions via advanced microscopy.

Material and Methods

Cloning of Split-HaloTag® Gateway destination vectors

The optimised HaloTag®-7 sequence (298 amino acids) from Promega (https://www.promega.de/) was genetically split on position 155/156 aa into the N-terminal fragment “NHalo” (aa 1-155) and the C-terminal fragment “CHalo” (aa 156-298) according to the initial experiment of Ischikawa and colleagues (2012). In order to create Split-HaloTag® GATEWAY® destination vectors, enabling C-terminal Split-HaloTag® reporter fusion, the binary destination vectors pDest- *Cluc*-GW and pDest-GW-*Cluc* were used (Gehl *et al.,* 2011). PCR-Primers were designed to fuse specific restriction enzyme recognition sequences at both reporter fragments (Table S1). After amplification, *Cluc* fragments were exchanged by restriction and ligation for *Nhalo* or *Chalo* residues using the restriction sites *Xba*I and *Spe*I (N-

terminal) and *Xho*I/*Sac*I (C-terminal), respectively (restriction enzymes purchased by Thermo Fischer Scientific (https://www.thermofisher.com)), to create pDest-*Nhalo*-GW, pDest-*GW-Nhalo,* pDest-*Chalo*-GW and pDest-*GW-Chalo* (Table S2).

Expression vectors

Coding sequences of Cnx6 (AT2G43760), Cnx7 (AT4G10100) and Map65 (amino acids 340–587; AT5G55230) were fused to Split-HaloTag® fragments via a two-step fusion PCR with Phusion-Polymerase purchased from Thermo Fischer Scientific (https://www.thermofisher.com). For the first PCR, each single cDNA and reporter fragment was created with an overlapping sequence to each, which enable assembly of fusion constructs (used primers listed in Table S1). For the second step, the products of the first PCR were assembled due to the overlapping matching sequences and then amplified a one single fragment. This *att*B-site flanked constructs were subcloned via BP-reaction into the Donor vector pDONR/Zeo to create entry vectors. Recombining these into pK7WG2 (Karimi *et al*., 2002) using LR-reactions generated the expression vectors pExp-*Nhalo-cnx7*, pExp-*Chalo- cnx6* and pExp-*Chalo-map65.*

All BiFC expression vectors and entry vectors with coding sequences of Cnx1 (AT5G20990), LA (amino acids 1–17 of the *Saccharomyces cerevisiae* protein ABP140), ABD2 (aminoacids 325–687; AT4G26700), CKL6 (amino acids 302–479; AT4G28540) and NLuc were available and are described by Kaufholdt *et al*. (2016a). The entry vectors were used to clone Split-HaloTag® expression vectors via LR-reactions into pDest-*GW-Nhalo* and pDest-*GW-Chalo* to create pExp-*cnx1-Nhalo,* pExp-*la-Nhalo,* pExp-*ckl6-Nhalo,* pExp-*la-Chalo,* pExp-*abd2-Chalo* and pExp-*Nluc-Chalo.*

Plant transformation

N. benthamiana wild type plants were cultivated in soil under greenhouse conditions. They were used for *Agrobacterium*-mediated transient transformation of fusion constructs 7 to 12 weeks after germination as described by Gehl and colleagues (2011). *Agrobacterium* strain C58C1/pMP90 carrying binary expression vectors were freshly grown (48 h at 28 °C) on solid CPY media (0.1% (w/v) yeast extract, 0.5% (w/v) casein peptone, 0.5% (w/v) sucrose, 2 mg/L $MgSO_4$ x $7H_2O$ (pH 7); add 1.5% w/v agar) containing rifampicin (50 mg/L) and gentamycin

(50 mg/L) as well as kanamycin (50 mg/L). Helper strain p19 (Voinnet *et al.*,2003) was grown on CPY medium containing rifampicin (50 mg/L) and kanamycin (50 mg/L). After growing for 20 h in 9 mL of liquid CPY at 200 rpm at 28 °C, cells transferred into fresh activation medium containing 10 mM MES/KOH (pH 5.6), 10 mM $MgCl_2$ and 150 µM acetosyringone. Each strain was diluted in activation media to an optical density of OD_{600} = 0.9 (final OD_{600} = 0.3). Then, three strains were mixed for each transformation: (i) One strain containing a NHalo construct, (ii) one strain containing a CHalo-construct and (iii) the helper strain p19. After incubation for 2 h at 50 rpm (28 °C), mixed *Agrobacterium* suspension were infiltrated into abaxial site of young but fully expanded leaves. Plants were incubated for 3-5 days in the green house.

Staining of *N. benthamiana* leaves discs with HaloTag® ligands

Staining protocol based on the work of Lang and colleagues (2006). Leaf discs of (6-10 mm) of *N. benthamiana* leaves were transferred into a 20 mL syringe with screw lid and infiltrated with 2-4 mL ligand solution (0.5, 1.0 or 2.0 µM TMR, DiAcFAM and Oregon Green in 10 mM MES/KOH (pH 5.6) and 10 mM $MgCl_2$). All dyes were purchased from Promega (https://www.promega.de/). Syringes with leaf discs were wrapped in aluminium foil and incubated for 0.5, 15, 30 or 60 min either on the work bench, on a tumbling shaker or on a rotary tube mixer. After staining, the samples were washed with 10 mL washing solution by closing the screw lid and moving the plunger up and down for 10 times. Washing steps were repeated with fresh washing solution 6-12 times. Furthermore, one duration before the last washing step of 0, 3 or 12 hours in washing solution was performed.

Confocal laser scanning microscopy

The confocal Laser Scanning Microscope LSM 510Meta from Zeiss (Göttingen, Germany) was used. The cLSM-510META scanhead was connected to the Axiovert 200M. All images were examined using either the Plan-Neofluar 10x/0.3 or the C-Apochromat 40x/1.2 water-immersion objective. For excitation, both an argon laser (488 nm for BiFC, Oregon Green and DiAcFAM as well as chlorophyll fluorescence) and a Helium-Neon Laser (543 nm line for TMR) was used. The emitted light passed the primary beam-splitting mirror UV/488/543/633 and was separated by a secondary beam splitter at 545 nm. Fluorescence was detected with filter sets as follows: BP 505-530 nm for BiFC (Em_{max}: 515 nm), Oregon Green (Em_{max}: 520 nm) and DiAcFAM (Em_{max}: 521 nm); BP 560-615 for TMR (Em_{max}: 578 nm); LP 650 nm for chlorophyll

fluorescence. Bright field images were taken with the transmitted light photomultiplier. The Lambda mode was used to examine the spectral signature of fluorophores. All images were taken using ZEISS Microscope Software ZEN 2009 and processed with ZEN lite and Fiji (Schindelin *et al*., 2012).

Super-resolution by polarisation demodulation microscopy

Principles of the experimental set-up are described by Hafi and colleagues (2014) and modifications enabling the analysis of the dye´s 3D-orientations were described by Albrecht *et al*. (2020). The cover slip was fixed to the microscope slide with nail polish and directly used for microscopy. Linearly polarised light deriving from a 488 nm continuous wave (CW) laser (sapphire 488-50, Coherent) was used for excitation of Oregon Green molecules. The beam was expanded through a telescope system. The polarisation was modulated at 15 frames per modulation period by rotation of a λ/2-waveplate. The rotation was achieved through a chopper wheel (Optical Chopper Systems, Thorlabs) which was synchronised to an electron-multiplying charge-coupled device (EMCCD) camera (iXonEM+897 back illuminated, Andor Technology). Through the rotation of 2 wedge prisms lateral shift of the beam was caused that enabled measurements of the fluorophores being excited from a different direction. Then, the beam was focused onto the back aperture of the microscope objective (UPlanSApo, 60×, NA = 1.35 oil immersion, Olympus), which was integrated in an inverted microscope body (IX 71, Olympus). Emitted light was then passed through a dichroic mirror (beam splitter z 488 RDC, AHF) and an emission filter (ET band pass 525/50, AHF). To further magnify the image and focus it the EMCCD camera an additional lenses system was used. During the measurement 2,000 frames at approximately 32 ms per frame were recorded. The first 200 frames were neglected for calibration purposes. The raw fluorescence intensity of all modulation periods of the last 1,800 frames of a measurement was used for analyses. Images were “deblurred” by using deconvolution algorithms. The “blurring” function or point-spread function (PSF) was approximated by using the PSF-Generator Plugin for ImageJ (http://bigwww.epfl.ch/algorithms/psfgenerator/). Using the PSF, the modulating fluorescence intensities were deblurred using an iterative least-squares deconvolution while accounting for the polarisation modulation. The least-squares functional was minimised by using the FISTA Algorithm (Beck and Teboulle, 2009).

Results and Discussion

The Split-HaloTag® constructs created in this study are based on the enhanced HaloTag®-7 sequence (298 amino acids), which has been optimised and improved with regard to solubility, stability, binding kinetics and access to an optional TEV-cleavage site (Ohana *et al*., 2009). It was split on position 155/156 aa into the N-terminal fragment "NHalo" (aa 1-155) and the C-terminal fragment "CHalo" according to the initial experiment of Ischikawa and colleagues (2012). The two amino acids important for covalent ligand binding are located on each of the two separate Split-HaloTag® fragments. The stable bond between HaloTag® protein and ligand is formed by the catalytic amino acid Asp^{106} as part of the "NHalo" fragment. Therefore, independent expression of "NHalo" or "CHalo" fragments will not enable ligand binding without each other (Fig. 1A/B), which is a fundamental aspect when using Split-HaloTag® imaging for investigation of protein-protein interactions. The cDNAs of the interaction partners were fused N- or C-terminaly to the NHalo and CHalo fragments via fusion PCR and gateway cloning (see Materials and Methods). For high flexibility, Split-HaloTag® GATEWAY compatible destination vectors were generated which enabled a fast and easy cloning of expression vectors with coding sequences of different proteins of interest.

Reconstitution of Split-HaloTag® *in planta*

The complex formation of the heterotetrameric molybdopterin synthase (MPT) subunits Cnx6 and Cnx7 from *Arabidopsis thaliana* was used to demonstrate the capability of reconstitution of the Split-HaloTag® *in planta*. This protein pair was chosen as positive control due to their verified high binding strength (Kaufholdt *et al*., 2013). The two interacting proteins (Fig. 1C) will bring the two HaloTag reporter fragments to close spatial proximity and, thereby, guide the reconstitution of functional HaloTag® proteins.

After transformation of *Nicotiana benthamiana* epidermis cells and staining with the fluorescent ligand TMR, specific cytoplasmic fluorescence was observed as a thin layer at the cell periphery (Fig. 1D). Wild type leaves were stained similarly, and lacking fluorescence signals indicated the washing steps being sufficient to remove unbound ligands (Fig. 1E). Therefore, since the MPT synthase complex is localised in the cytoplasm, HaloTag® fragments CHalo and NHalo were capable of reconstitution. In addition to the orange fluorescent ligand TMR, the ligands Oregon Green (green) as well as DiAcFAM (yellow) were able to bind (data

not shown), even though DiAcFAM signals were weaker as compared to TMR and Oregon Green.

After proving the general capability of Split-HaloTag® fragment reconstitution, this new assay was tested in a second approach including proteins attached to cytoskeleton structures such as filamentous (F-) actin as well as microtubules. By applying this approach, it was possible to test whether the Split-HaloTag® system allows for investigating the assembly of different proteins at cytoskeletal elements. Both structures were not labelled directly to NHalo or CHalo termini, but via binding proteins, as a fusion of larger reporter fragments directly to globular actin or tubulin proteins might disturb their polymerisation processes. For F-actin labelling, the binding domain of fimbrin from *A. thaliana* (ABD2; Sano *et al*., 2005) as well as of Abp140 from *Saccharomyces cerevisiae* (Lifeact/LA; Riedl *et al*., 2008) were used. Furthermore, microtubule binding domains of the two proteins Casein-Kinase-1-Like-6 (CKL6; Ben-Nissan *et al*., 2008) and the Microtubule Associated Protein 65 (Map65; Hamada, 2007) from *A. thaliana* were investigated. The cytoskeleton binding proteins show no direct protein interactions to each other. However, their affinity and subsequent binding and anchoring to the cytoskeletal structures results in such spatial proximity that it is able to act as model for a direct interaction of a cytoskeleton associated protein complex.

Expression of F-actin binding protein constructs followed by HaloTag® reconstitution and staining resulted in a TMR specific fluorescence visible as transversely arranged filaments with branches distributed throughout the cytoplasm (Fig. 1F). The approach with CLK6-NHalo and CHalo-Map65 to label microtubules upon Split-HaloTag® reconstitution displayed filamentous structures more equally distributed throughout the cell with less cross bridges compared to actin filaments (Fig. 1G). These structures are typical for F-actin and microtubules, respectively, which were observed in BiFC experiments before (Kaufholdt *et al*., 2016a). In all interaction approaches both actin filaments as well as microtubules, could successfully be visualised upon interaction of cytoskeletal binding proteins. It has to be noted that staining and washing procedure can cause severe stress and damage to the cells which will result in condensed and thicker actin filaments and microtubules, respectively.

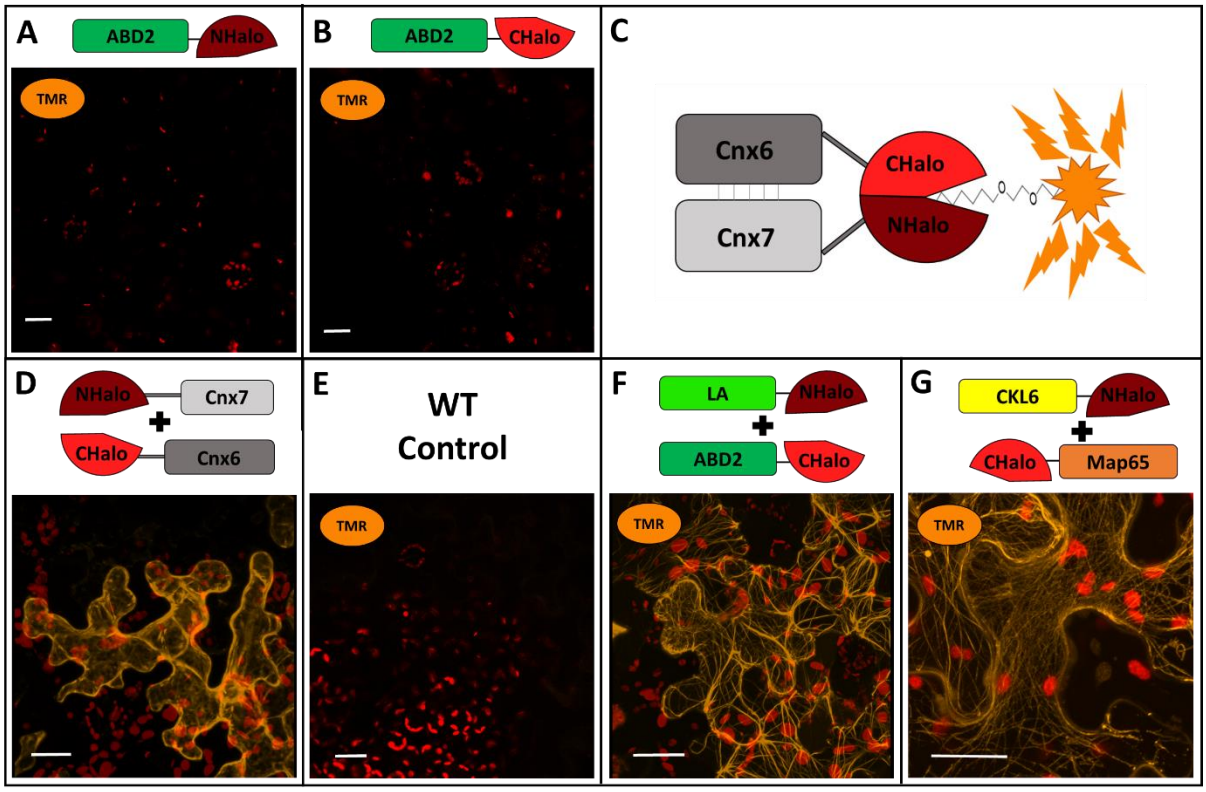

Fig. 1: Testing Split-HaloTag® complementation upon protein interactions of MPT synthase complex as well as at cytoskeleton binding proteins.

Shown are images of *N. benthamiana* epidermis cells via confocal microscopy detecting TMR. Staining of leaf discs was performed 4-5 days after transformation. All images were taken with a C-Apochromat 40x/1.2 water immersion objective. Scale bars depict a length of 20 µm each. **(A)** Negative controls of single transformed Split-HaloTag® reporter constructs fused to ABD2. **(C)** Schematic illustration of Split-HaloTag® reconstitution guided by the MPT synthase subunits Cnx6 and Cnx7 **(D)** Cytosolic TMR fluorescence after transformation with NHalo-Cnx7 and Cnx6-CHalo. **(E)** Negative control of a wildtype (WT) leaf after staining. **(F)** TMR fluorescence at actin after transformation of actin binding constructs LA-NHalo and ABD2-CHalo. **(G)** TMR fluorescence at microtubules filaments after transformation of microtubules binding constructs CKL6-NHalo and CHalo-Map65.

Insights into the Staining Protocol

It has been described by Lang and colleagues (2006), who first introduced the HaloTag® system to plant cells, that especially destaining procedures are of great importance to reduce unspecific background fluorescence. For interaction studies, comparison of fluorescence intensity and fluorescence pattern is the main task, where each form of background will falsify the result. However, after using the published destaining protocol an excess of unbound dye remained in the tissue. Therefore, optimised staining and destaining procedures had to be

established. To improve staining protocols and to evaluate the best HaloTag® ligand several different factors were investigated: (i) the size of analysed leaf discs, (ii) concentration of ligands, (iii) ligand incubation time, (iv) number of subsequent washing steps, (v) incubation time in washing solution and (vi) aeration of leaf discs in washing solution.

During this optimisation process, several general observations were made. After TMR staining, fluorescence was always detected in vascular tissue of transformed as well as wild type leaves suggesting a nonspecific adhesion between TMR and molecules in leaf veins (Fig. 2A). Furthermore, staining with more than 0.5 µM TMR combined with an insufficient number of washing steps resulted in oversaturation and accumulation of unbound dye in the cytoplasm of parenchyma cells (Fig. 2B). This amount of unbound TMR accumulation increased when using larger or damaged leaf discs or older plants. Moreover, recycling of frozen TMR solution led to unspecific aggregations inside the cells.

DiAcFAM staining gained an overall weaker fluorescence signal compared to TMR but no staining of vascular tissue was observed (not shown). However, weak DiAcFAM signals (Em_{max} 521 nm) could easily be mistaken for typical plant background fluorescence at approx. 530 nm. Furthermore, accumulation of unbound ligands occurred especially in stomata after DiAcFAM (Fig. 2C) but also after Oregon Green (Fig. 2D) staining. Therefore, DiAcFAM was excluded from further studies. In addition, Oregon Green resulted in accumulation inside vacuoles of parenchyma cells if incubated more than a few seconds in staining solution (Fig. 2E).

Optimal results for TMR staining were obtained using leaf discs of a diameter of 6-8 mm, a final TMR concentration of 0.5 µM in 2 mL fresh staining solution, 15 min incubation time and followed by eight subsequent washing steps into a 20 mL syringe and an overnight incubation in washing solution. Samples were incubated with 10 mL washing solution by closing the screw lid and moving the plunger up and down for approx. 10 times. Immediately before microscope analysis two more washing steps were performed. Both, overnight incubations either on a tumbling shaker or on a rotary tube mixer were equally sufficient for all dyes, as long as there was sufficient air in the syringe to allow leaf disc aeration.

Oregon Green showed optimal results if a 0.5 µM staining solution was exchanged with 2 mL washing solution immediately after its infiltration and incubated for 15 minutes. Then, the

washing procedure was applied as described for TMR. This could reduce but not completely avoid Oregon Green accumulation.

From all three tested dyes, TMR was the brightest, showing the least drawbacks. However, even after prolonged overnight incubation in repeatedly refreshed washing solution TMR was still bound to vascular tissue. Therefore, leaf area further away from vascular tissue should be used. Overall, TMR showed the best applicability for usage within a Split-HaloTag® complementation assay for staining *N. benthamiana* leaf discs.

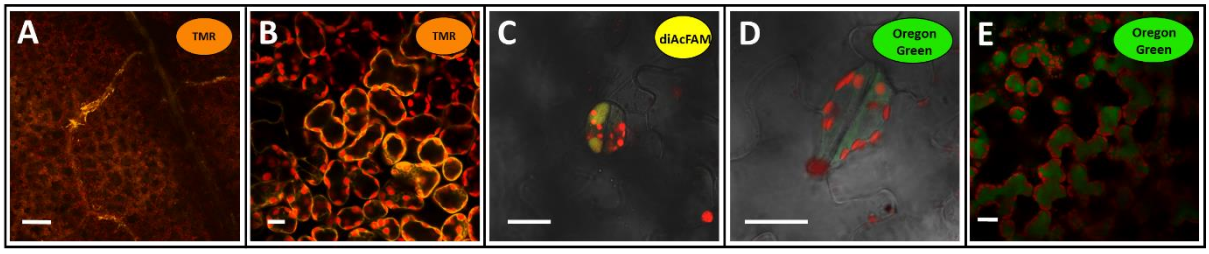

Fig. 2: Evaluation of HaloTag® fluorescent Ligands TMR, DiAcFAM and Oregon Green.
Confocal microscopy of *N. benthamiana* leaf discs stained with TMR **(A/B)**, DiAcFAM **(C)** or Oregon Green **(D/E)**. Images were taken either with a Plan-Neofluar 10x/0.3 **(A)** or with a C-Apochromat 40x/1.2 water immersion objective **(B-E)**. Scale bars depict a length of 100 µm **(A)** or 20 µm **(B-E)**. **(A)** Unspecific TMR binding in vascular tissue. **(B)** Oversaturation of unbound TMR in parenchyma cells after using 2 µM dye. **(C/D)** Accumulation of unbound ligands in stomata after DiAcFAM **(C)** and Oregon Green **(D)** staining. **(E)** Accumulation of unbound Oregon Green in parenchyma cells.

Validation of Split-HaloTag® imaging upon protein-protein interaction at actin filaments

After proving the general capability of Split-HaloTag® fragment reconstitution, we aimed at validating this new assay via a well-established interaction approach with a protein complex binding to F-actin. Kaufholdt *et al*. (2016a) successfully showed via BiFC that molybdenum insertase Cnx1 interacts with filamentous actin. Furthermore, it was shown that the whole Moco biosynthesis complex is anchored to actin filaments through the G-domain of Cnx1.

This well-established interaction was used to investigate whether Split-HaloTag® fragments will reconstitute only upon interaction of two fused proteins or also unspecifically by chance and diffusion. Therefore, *in vivo* protein-protein interaction studies require adequate negative controls as described by Kaufholdt *et al*. (2016b). As negative control protein, the cytosolic

protein NLuc (N-terminus of the luciferase from *Photinus pyralis*) was provided, which had no interaction with the analysed proteins of interest (Gehl *et al*., 2011).

In the interaction approach, reporter fusion constructs of Cnx1 and the actin binding protein LA, respectively, were co-expressed in *N. benthamiana*. For comparison, the BiFC approach was included, for which the reporter halves VYNE (N-terminus of Venus) and SCYCE (C-terminus of SCFP) were used (Gehl *et al*., 2009). Both BiFC and Split-HaloTag® complementation assay show almost identical results (Fig. 3 A/B). Both TMR and GFP fluorescence were detected in a filamentous pattern concentrated at the actin nucleus basket and thinned out at F-actin towards the cellular cortex. A typical pattern for studying an actin interacting protein complex was observed in both approaches that is reminiscent of a "starry sky" (Kaufholdt *et al*., 2016a). When LA-NHalo was co-expressed with NLuc-CHalo in the negative control, TMR specific fluorescence at actin filaments was detected, too. This background fluorescence is caused by reconstitution by chance in the small cytosolic space, which is typical for split-protein assays in plant cells (Gehl *et al*., 2009/2011). A negative control without any fluorescence would be an unrealistic event, which should be verified by an additional abundance control (Kaufholdt *et al*., 2016b). However, the TMR fluorescence was equally distributed within the cell and no starry sky could be observed (Fig. 3C). Therefore, the characteristic starry sky like pattern of the interaction approach with Cnx1 demonstrate its interaction with F-actin. Both BiFC and Split-HaloTag® assay showed almost identical results, which proves the applicability of the Split-HaloTag® system to investigate associations of different proteins to the cytoskeleton.

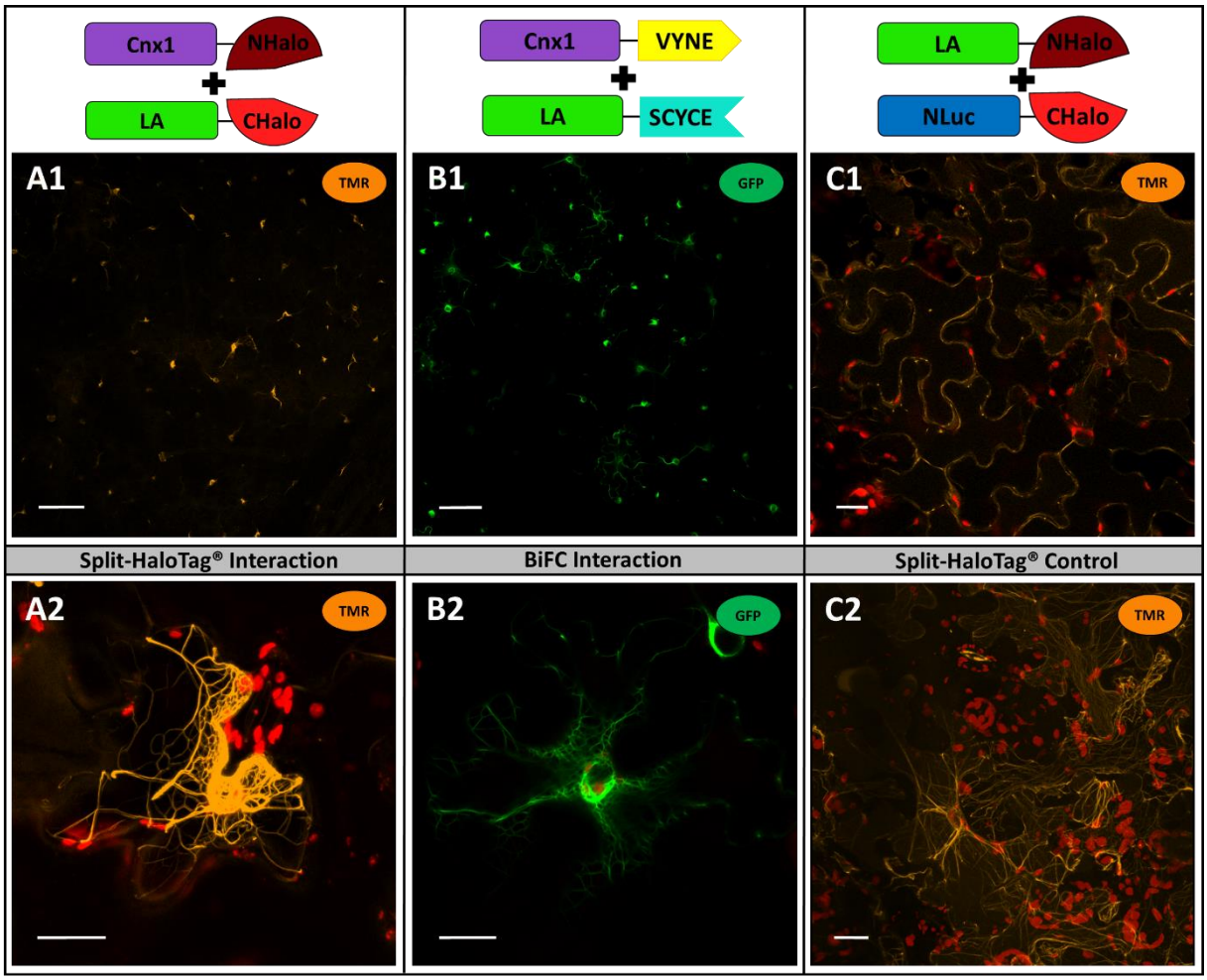

Fig. 3: Split-HaloTag® Protein-Protein Interaction Studies of Cnx1 and Actin Filaments via Lifeact. Shown are images of *N. benthamiana* epidermis cells via confocal microscopy of TMR or GFP. Staining of leaf discs was performed 4-5 days after transformation. All images were taken with a Plan-Neofluar 10x/0.3 **(A1/B1/C1)** or with a C-Apochromat 40x/1.2 water immersion objective **(A2/B2/C2).** Scale bars depict a length of 100 µm **(A1/B1/C1)** or 20 µm **(A2/B2/C2)**. **(A)** Split-HaloTag® approach with Cnx1-NHalo and LA-CHalo. **(B)** BiFC approach with Cnx1-VYNE and LA-SCYCE. **(C)** Corresponding Split-HaloTag® negative control where Cnx1 was replaced by the independent protein NLuc. **(A)** and **(B)** were imaged with identical setting for optimal comparison of strength and pattern.

Application examples of Split-HaloTag® for 3D-images and subdiffractional polarisation imaging.

The Split-HaloTag® imaging assay has been proven as a feasible method for imaging of protein interactions. However, conventional light and fluorescence microscopy are diffraction-limited to a resolution limit of approx. 200 nm in the lateral (x-y) and about 600 nm in the axial (z) direction (Cremer and Masters, 2013). Many subcellular structures are smaller which hampers

their detailed observation (Huang *et al*., 2009). To circumvent these restrictions, advanced fluorescence imaging methods such as single molecule detection, subdiffractional polarisation imaging or super-resolution microscopy (SRM) techniques have been developed to improve the resolution and to allow studying molecular processes more detailed (Moerner and Kador 1989; Orrit and Bernard, 1990; Bode *et al*., 2008; Holleboom *et al*., 2014; Liao *et al*., 2010/2011; Godin *et al*., 2014; Loison *et al*., 2018; Camacho *et al*., 2019). However, stable fluorescence molecules are needed for such advanced imaging techniques which is hard to realise by standard fluorescence proteins. The Split-HaloTag® system has the advantage of using several stable dyes emitting light at various wavelength. Liss *et al*. (2015) for example used HaloTag® and a TMR ligand successfully in animal cell cultures for correlative light and electron microscopy (CLEM) of protein dynamics with ultrastructure details. Reck-Peterson and colleagues (2006) used the HaloTag® to label dynein in sea urchin axonemes and tracked single molecules with a precision of a few nanometers to reveal dynein´s stepping behaviour at microtubules. Small organic fluorophores can be used in variable dosages to label only a few molecules and are available with different spectral behavior. Moreover, several organic fluorophores especially for live-cell labelling and subsequent imaging were recently developed with photoactivatable properties (Lee *et al.,* 2010) as well as with improved quantum efficiency and superior brightness while retaining excellent cell permeability (Grimm *et al*., 2015).

As a first approach, interaction of Cnx1 and the actin binding protein ABD2 were performed to show the potential of stable TMR fluorescence for 3D-images at confocal laser scanning microscopy. For this purpose, each layer of a cell has to be scanned in very thin optical slices (µm range or less). Such a detailed imaging can take several minutes, which leads to high damages through photo bleaching at standard fluorescence proteins. However, the stable TMR fluorescence of a Split-HaloTag® enabled more defined results of 3D cell images (Fig. 4A) compared to BiFC approaches (Fig. 4B), which is demonstrated by the very thin filaments of actin network hardly detectable by BiFC.

Super-resolution by polarisation demodulation (SPoD) microscopy was used as second example for demonstrating the performance of the Split-HaloTag® system. This advanced fluorescence imaging technique is a subdiffractional polarisation imaging method that allows measurement of the average orientation of fluorescent dyes attached to different structures

and was first described by Hafi and colleagues (2014). Fluorescent molecules are illuminated via linearly polarised light. This causes the fluorophores to be excited at different times, which results in a modulated fluorescence intensity from the fluorophores. Depending on the orientation of the illuminated fluorophores (or more specifically the orientation of their transition dipole moments), the observed fluorescence intensity will be phase-shifted, and differently oriented fluorophores will emit periodic signals peaking at different points in time. With subsequent analysis via deconvolution algorithms it was tested whether structures at subdiffractional distances can be separated by different fluorescence polarisations. During each measurement, 2,000 frames were recorded, which in itself is not problematic when using stable dyes. Split-HaloTag® constructs with the two microtubule binding domains of CLK6 and Map65 were used for this purpose. Overexpression of MAP65 isotypes is known to result in microtubule bundling (Mao *et al*. 2006). After transformation and expression, leaf discs were stained with Oregon Green, which fluorescence was more appropriate for SPoD microscopy. . The observed fluorescence resulted in individual microtubules (Fig. 4B1). Albeit high amounts of background fluorescence and out-of-focus signal complicated the recording and modulation analysis, subdiffractional separation in a branching region of distinct fibres was observed in the deconvolved image (Fig. 4B2) and was supported by different phases as visualised by a simple red/green colour code. These different phases in the branching region of the two fibres were already observable in the raw modulation data. Certainly, future work is needed to enhance separation by different phases in addition to pure image deconvolution for entire cell images. Nevertheless, Split-HaloTag® imaging assay can be used for such advanced fluorescence imaging techniques.

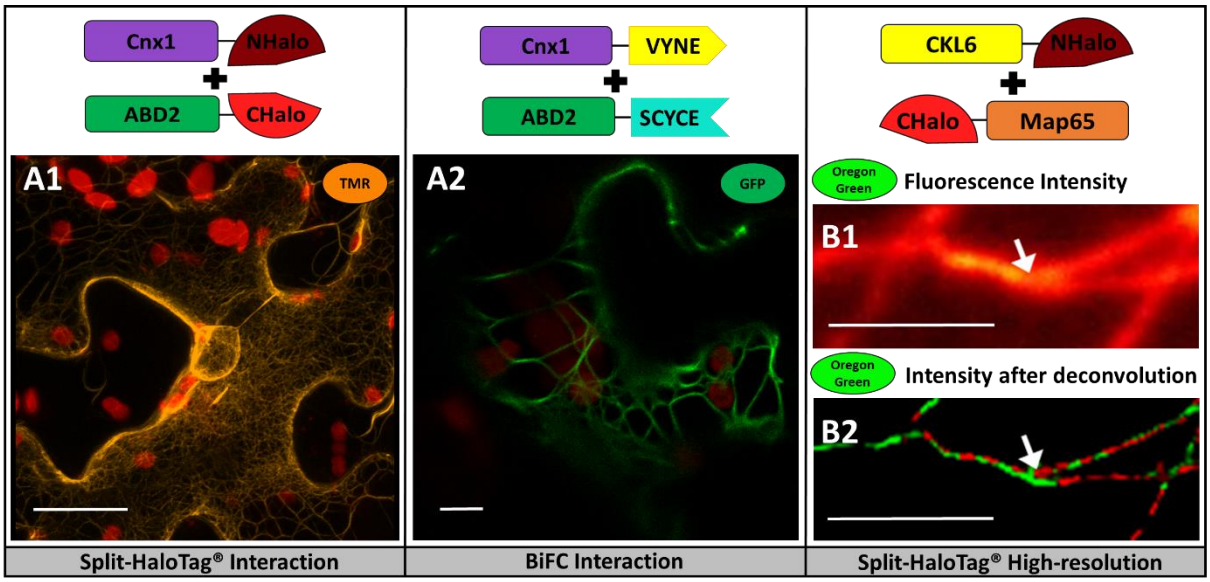

Fig. 4: Analysis of Split-HaloTag® images via confocal 3D-microscopy and super-resolution SPoD microscopy.

Shown are *N. benthamiana* cells three days after transformation. **(A)** Interaction approaches at actin filaments with Cnx1 and ABD2 via Split-HaloTag® **(A1)** or BiFC **(A2)**. Split-HaloTag® Staining was performed with TMR. Images were taken with a C-Apochromat 40x/1.2 water immersion objective. Scale bars depict a length of 20 µm. **(B)** SPoD microscopy of microtubules stained with Oregon Green after transformation of the Split-HaloTag® microtubules binding constructs CKL6-NHalo and CHalo-Map65. **(B1)** Diffraction limited image depicting averaged raw fluorescence intensity. **(B2)** Phase color coded fluorescence intensity image after 1000 iterations of the deconvolution algorithm. The red/green colorcode support subdiffractional separation of the fibers at a distinct branching fork (arrow) that is not visible in the conventional diffraction of wide field image. However, future work is needed to enhance separation by different phases in addition to pure image deconvolution for entire cell images. The raw data scale bars depict 2 µm each.

Conclusion

In this study, the Split-HaloTag® imaging assay was established for the first time *in planta*. Vectors were cloned and reporter termini NHalo and CHalo were tested for reconstitution in both fusion orientations to the protein of interest and in all four orientation combinations to each other. The applicability of the system for interaction studies was demonstrated by means of the Molybdenum cofactor biosynthesis complex anchoring to F-actin. The advantage of the Split-HaloTag® system lies in the ability to visualise specific protein interactions in advanced imaging techniques such as 3D, polarisation, single-molecule or super-resolution imaging

methods that require brighter and more stable fluorescence markers. Localisation of protein complexes can be observed with the split-HaloTag® imaging assay in a distinct manner. In live-cell microscopy, the method combines *in vivo* split-reporter analyses with the HaloTag® advantages of a huge set of differently coloured fluorescent ligands, their photostability compared to fluorescence proteins and the ability to vary labelling intensity via dosage of dyes independent from protein expression. Therefore, this assay is a new tool for 3D-imaging and super-resolution microscopy of protein-protein interactions in plant cells.

Supplemental information

Supplemental data are available online.

Table S1: Primers for Cloning and sequencing of Split-HaloTag® related constructs and vectors.

Table S2: Split-HaloTag® Destination and Expression vectors used within this work.

Acknowledgement

We are grateful to Dr. Christin-Kirsty Baillie for scientific support and critical reading. We thank Tanja Linke for excellent technical work in our lab. This work was financially supported by the Deutsche Forschungsgemeinschaft (grant GRK2223/1) to RH and RRM.

Author Contribution

RMe, HB, PJW, RRM, RH and DK planned and designed the project. RMe, JNW, MB, CT, SF, JS and DK cloned the vectors, performed plant transformation and the cLSM experiments. AA and RMa handled SPoD microscopy. All authors analysed and discussed the results. RMe, JNW, RH and DK were primarily involved in drafting the manuscript and RMe and DK produced figures and tables. JS, HR, PJW and RRM critically read the manuscript and improved the text, all authors finalised it. RH and DK coordinated the work.

References

Albrecht A, Pfennig D, Nowak J, Matis R, Schaks M, Hafi N, Rottner K, Walla, PJ. 2020. Amplitude Analysis of Polarization Modulation Data and 3D-Polarization Demodulation (3D-SPoD). *bioRxiv*. https://doi.org/10.1101/2020.03.10.986034.

Beck A, Teboulle M. 2009. A fast iterative shrinkage-thresholding algorithm with application to wavelet-based image deblurring. In 2009 IEEE International Conference on Acoustics, Speech and Signal Processing, pp. 693-696.

Ben-Nissan G, Cui W, Kim DJ, Yang Y, Yoo BC, Lee JY. 2008. Arabidopsis casein kinase 1-like 6 contains a microtubule-binding domain and affects the organization of cortical microtubules. Plant physiology, 148(4), 1897-1907.

Bhat RA, Lahaye T, Panstruga R. 2006. The visible touch: in planta visualization of protein-protein interactions by fluorophore-based methods. Plant methods, 2(1), 12.

Bode S, Quentmeier CC, Liao PN, Barros T, Walla PJ. 2008. Xanthophyll-cycle dependence of the energy transfer between carotenoid dark states and chlorophylls in NPQ mutants of living plants and in LHC II. Chemical Physics Letters, 450(4-6), 379-385.

Camacho R, Täuber D, Scheblykin IG. 2019. Fluorescence Anisotropy Reloaded—Emerging Polarization Microscopy Methods for Assessing Chromophores' Organization and Excitation Energy Transfer in Single Molecules, Particles, Films, and Beyond. *Advanced Materials*, *31*(22), 1805671.

Cremer C, Masters BR. 2013. Resolution enhancement techniques in microscopy. The European Physical Journal H, 38(3), 281-344.

England CG, Luo H, Cai W. 2015. HaloTag technology: a versatile platform for biomedical applications. Bioconjugate chemistry, 26(6), 975-986.

Gehl C, Waadt R, Kudla J, Mendel RR, Hänsch R. 2009. New GATEWAY vectors for high throughput analyses of protein–protein interactions by bimolecular fluorescence complementation. Molecular plant, 2(5), 1051-1058.

Gehl, C, Kaufholdt D, Hamisch D, Bikker R, Kudla J, Mendel RR, Hänsch R. 2011. Quantitative analysis of dynamic protein–protein interactions in planta by a floated-leaf luciferase complementation imaging (FLuCI) assay using binary Gateway vectors. The Plant Journal, 67(3), 542-553.

Godin AG, Lounis B, Cognet L. 2014. Super-resolution microscopy approaches for live cell imaging. Biophysical journal, 107(8), 1777-1784.

Grimm JB, English BP, Chen J, Slaughter JP, Zhang Z, Revyakin A, Patel R, Macklin JJ, Normanno D, Singer RH, Lionnet T, Lavis LD. 2015. A general method to improve fluorophores for live-cell and single-molecule microscopy. Nature methods, 12(3), 244.

Hafi N, Grunwald M, Van Den Heuvel LS, Aspelmeier T, Chen JH, Zagrebelsky M, Schütte OM, Steinem C, Korte M, Munk A, Walla PJ. 2014. Fluorescence nanoscopy by polarization modulation and polarization angle narrowing. Nature methods, 11(5), 579.

Hamada T. 2007. Microtubule-associated proteins in higher plants. Journal of plant research, 120(1), 79-98.

Holleboom CP, Walla PJ. 2014. The back and forth of energy transfer between carotenoids and chlorophylls and its role in the regulation of light harvesting. Photosynthesis research, 119(1-2), 215-221.

Huang B, Bates M, Zhuang X. 2009. Super-resolution fluorescence microscopy. Annual review of biochemistry, 78, 993-1016.

Ishikawa H, Meng F, Kondo N, Iwamoto A, Matsuda Z. 2012. Generation of a dualfunctional split-reporter protein for monitoring membrane fusion using self-associating split GFP. Protein Engineering, Design & Selection, 25(12), 813-820.

Karimi M, Inzé D, Depicker A. 2002. GATEWAY™ vectors for Agrobacterium-mediated plant transformation. Trends in plant science, 7(5), 193-195.

Kaufholdt D, Gehl C, Geisler M, Jeske O, Voedisch S, Ratke C, Bollhöner B, Mendel RR, Hänsch R. 2013. Visualization and quantification of proteininteractions in the biosynthetic pathway of molybdenum cofactor in *Arabidopsis thaliana*. J. Exp. Bot. 64, 2005–2016.

Kaufholdt D, Baillie CK, Bikker R, Burkart V, Dudek CA, von Pein L, Rothkegel M, Mendel RR, Hänsch R. 2016a. The molybdenum cofactor biosynthesis complex interacts with actin filaments via molybdenum insertase Cnx1 as anchor protein in Arabidopsis thaliana. Plant Science, 244, 8-18.

Kaufholdt D, Baillie CK, Meyer MH, Schwich OD, Timmerer UL, Tobias L, van Thiel D, Hänsch R Mendel RR. 2016b. Identification of a protein-protein interaction network downstream of molybdenum cofactor biosynthesis in Arabidopsis thaliana. Journal of plant physiology, 207, 42-50.

Kaufholdt D, Baillie CK, Meinen R, Mendel RR, Hänsch R. 2017. The Molybdenum Cofactor Biosynthesis Network: In vivo Protein-Protein Interactions of an Actin Associated Multi-Protein Complex. Frontiers in plant science, 8, 1946.

Kerppola TK. 2013. Bimolecular fluorescence complementation (BiFC) analysis of protein interactions in live cells. Cold Spring Harbor Protocols, 2013(8), pdb-prot076497.

Lang C, Schulze J, Mendel RR, Hänsch R. 2006. HaloTag™: A new versatile reporter gene system in plant cells. Journal of experimental botany, 57(12), 2985-2992.

Lee HLD, Lord SJ, Iwanaga S, Zhan K, Xie H, Williams JC, Wang H, Bowman GR, Goley ED, Shapiro L, Twieg RJ, Rao J, Moerner WE. 2010. Superresolution imaging of targeted proteins in fixed and living cells using photoactivatable organic fluorophores. Journal of the American Chemical Society, 132(43), 15099-15101.

Liao PN, Bode S, Wilk L, Hafi N, Walla PJ. 2010. Correlation of electronic carotenoid–chlorophyll interactions and fluorescence quenching with the aggregation of native LHC II and chlorophyll deficient mutants. Chemical Physics, 373(1-2), 50-55.

Liao PN, Pillai S, Gust D, Moore TA, Moore AL, Walla PJ. 2011. Two-Photon Study on the Electronic Interactions between the First Excited Singlet States in Carotenoid− Tetrapyrrole Dyads. The Journal of Physical Chemistry A, 115(16), 4082-4091.

Liss V, Barlag B, Nietschke M, Hensel M. 2015. Self-labelling enzymes as universal tags for fluorescence microscopy, super-resolution microscopy and electron microscopy. Scientific reports, 5, 17740.

Loison O, Weitkunat M, Kaya-Çopur A, Alves CN, Matzat T, Spletter ML, Luschnig S, Brasselet S, Lenne PF, Schnorrer F. 2018. Polarization-resolved microscopy reveals a muscle myosin motor-independent mechanism of molecular actin ordering during sarcomere maturation. PLoS biology, 16(4), e2004718.

Los G, Wood K. 2007. The HaloTag: A novel technology for cell imaging and protein analysis. Methods. Mol. Biol. 356, 195–208.

Los GV, Encell LP, McDougall MG, Hartzell DD, Karassina N, Zimprich C, Wood MG, Learish R, Ohana RF, Urh M, Simpson D, Mendez J, Zimmermann K, Otto P, Vidugiris G, Zhu J, Darzins A, Klaubert DH, Bulleit RF, Wood KV. 2008. HaloTag: a novel protein labeling technology for cell imaging and protein analysis. ACS chemical biology, 3(6), 373-382.

Mao G, Buschmann H, Doonan JH, Lloyd CW. 2006. The role of MAP65-1 in microtubule bundling during Zinnia tracheary element formation. Journal of cell science, 119(4), 753-758.

Miyawaki A, Sawano A, Kogure T. 2003. Lighting up cells: labelling proteins with fluorophores. Nat Cell Biol., S1-S7.

Moerner WE, Kador L. 1989. Optical detection and spectroscopy of single molecules in a solid. Physical review letters, 62(21), 2535.

Morisaki T, McNally JG. 2014. Photoswitching-Free FRAP Analysis with a Geneticall Encoded Fluorescent Tag. PLoS ONE, 9(9), e107730

Ohana RF, Encell LP, Zhao K, Simpson D, Slater MR, Urh M, Wood KV. 2009. HaloTag7: a genetically engineered tag that enhances bacterial expression of soluble proteins and improves protein purification. Protein expression and purification, 68(1), 110-120.

Orrit M, Bernard J. 1990. Single pentacene molecules detected by fluorescence excitation in a p-terphenyl crystal. Physical review letters, 65(21), 2716.

Reck-Peterson SL, Yildiz A, Carter AP, Gennerich A, Zhang N, Vale RD. 2006. Single-molecule analysis of dynein processivity and stepping behavior. Cell, 126(2), 335-348.

Riedl J, Crevenna AH, Kessenbrock K, Yu JH, Neukirchen D, Bista M, Bradke F, Jenne D, Holak TA, Werb Z, Sixt M, Wedlich-Soldner R. 2008. Lifeact: a versatile marker to visualize F-actin. Nature methods, 5(7), 605.

S**ano T, Higaki T, Oda Y, Hayashi T, Hasezawa S.** 2005. Appearance of actin microfilament 'twin peaks' in mitosis and their function in cell plate formation, as visualized in tobacco BY-2 cells expressing GFP–fimbrin. The Plant Journal, 44(4), 595-605.

Schindelin J, Arganda-Carreras I, Frise E, Kaynig V, Longair M, Pietzsch T, Preibisch S, Rueden C, Saalfeld S, Schmid B, Tinevez JY, White DJ, Hartenstein V, Eliceiri K, Tomancak P, Cardona A. 2012. Fiji: an open-source platform for biological-image analysis. Nature methods, 9(7), 676-682.

Voinnet O, Rivas S, Mestre P, Baulcombe D. 2003. An enhanced transient expression system in plants based on suppression of gene silencing by the p19 protein of tomato bushy stunt virus. Plant J. 33, 949–956.

Zitnik M, Feldman MW, Leskovec J. 2019. Evolution of resilience in protein interactomes across the tree of life. Proceedings of the National Academy of Sciences, 116(10), 4426-4433